Direct Imaging Detection of Methane in the Atmosphere of GJ 504 b

Markus Janson[1,2], Timothy D. Brandt[2], Masayuki Kuzuhara[3,4], David S. Spiegel[5], Christian Thalmann[6], Thayne Currie[7], Michael Bonnefoy[8], Neil Zimmerman[8], Satoko Sorahana[9], Takayuki Kotani[4], Joshua Schlieder[8], Jun Hashimoto[4], Tomoyuki Kudo[10], Nobuhiko Kusakabe[4], Lyu Abe[11], Wolfgang Brandner[8], Joseph C. Carson[12], Sebastian Egner[10], Markus Feldt[8], Miwa Goto[13], Carol A. Grady[14,15], Olivier Guyon[10], Yutaka Hayano[10], Masahiko Hayashi[4], Saeko Hayashi[10], Thomas Henning[8], Klaus W. Hodapp[16], Miki Ishii[10], Masanori Iye[4], Ryo Kandori[4], Gillian R. Knapp[2], Jungmi Kwon[17], Taro Matsuo[18], Michael W. McElwain[14], Kyle Mede[3], Shoken Miyama[19], Jun-Ichi Morino[4], Amaya Moro-Martín[20], Takao Nakagawa[21], Tetsuro Nishimura[10], Tae-Soo Pyo[10], Eugene Serabyn[22], Takuya Suenaga[17], Hiroshi Suto[4], Ryuji Suzuki[23], Yasuhiro Takahashi[24], Michihiro Takami[25], Naruhisa Takato[10], Hiroshi Terada[10], Daego Tomono[10], Edwin L. Turner[2,26], Makoto Watanabe[27], John Wisniewski[28], Toru Yamada[29], Hideki Takami[10], Tomonori Usuda[10], Motohide Tamura[4,17]

ABSTRACT

Most exoplanets detected by direct imaging so far have been characterized by relatively hot ($\gtrsim$1000 K) and cloudy atmospheres. A surprising feature in some of their atmospheres has been a distinct lack of methane, possibly implying non-equilibrium chemistry. Recently, we reported the discovery of a planetary companion to the Sun-like star GJ 504 using Subaru/HiCIAO within the SEEDS survey. The planet is substantially colder (<600 K) than previously imaged planets, and has indications of fewer clouds, which implies that it represents a new class of planetary atmospheres with expected similarities to late T-type brown dwarfs in the same temperature range. If so, one might also expect the presence of significant methane absorption, which is characteristic of such objects. Here, we report the detection of deep methane absorption in the atmosphere of GJ 504 b, using the Spectral Differential Imaging mode of HiCIAO to distinguish the absorption feature around 1.6 μm. We also report updated JHK photometry based on new K_s-band data and a re-analysis of the existing data. The results support the notion that GJ 504 b has atmospheric properties distinct from other imaged exoplanets, and will become a useful reference object for future planets in the same temperature range.

Subject headings: planetary systems — stars: solar-type — techniques: photometric

[1] Astrophysics Research Centre, Queen's University Belfast, University Road, BT7 1NN Belfast, Northern Ireland, UK; m.janson@qub.ac.uk

[2] Department of Astrophysical Sciences, Princeton University, NJ 08544, USA

[3] Department of Earth and Planetary Science, The University of Tokyo, 7-3-1 Hongo, Bunkyo-ku, Tokyo 113-0033, Japan

[4] National Astronomical Observatory of Japan, 2-21-1 Osawa, Mitaka, Tokyo 181-8588, Japan

[5] Astrophysics Department, Institute for Advanced Study, Princeton, NJ 08540, USA

[6] Institute for Astronomy, ETH Zurich, Wolfgang-Pauli-Strasse 27, CH-8093 Zurich, Switzerland

[7] Department of Astronomy and Astrophysics, University of Toronto, 50 St George Street, Toronto, ON M5S 3H8, Canada

[8] Max Planck Institute for Astronomy, Königstuhl 17, 69117 Heidelberg, Germany

[9] Division of Particle and Astrophysical Science, Nagoya University, Furo-Cho, Chikusa, Nagoya 464-8602, Japan

[10] Subaru Telescope, 650 North Aohoku Place, Hilo, HI 96720, USA

[11] Laboratoire Lagrange, UMR7239, University of Nice-Sophia Antipolis, CNRS, Observatoire de la Cote d'Azur, 06300 Nice, France

[12] Department of Physics and Astronomy, College of Charleston, 58 Coming Street, Charleston, SC 29424, USA

1. Introduction

Several companions to stars in or near the planetary regime have been discovered through direct imaging in recent years (e.g. Marois et al. 2010; Lagrange et al. 2010; Carson et al. 2013), which has provided the opportunity for characterization of their atmospheres. The HR 8799 system in particular has been the subject of several studies using spectroscopy and multi-band photometry. These observations have provided indications of atmospheric properties such as non-equilibrium chemistry (e.g. Janson et al. 2010; Hinz et al. 2010; Bowler et al. 2010) and thick clouds (e.g. Barman et al. 2011; Currie et al. 2011; Skemer et al. 2012). The latter implies that there may be a difference in cloud retention between ∼1000 K planets and more massive brown dwarfs in the same temperature range. Brown dwarfs undergo the so-called L/T transition

[13]Universitäts-Sternwarte München, Ludwig-Maximilians-Universität, Scheinerstr. 1, 81679 Munich, Germany

[14]Exoplanets and Stellar Astrophysics Laboratory, Code 667, Goddard Space Flight Center, Greenbelt, MD 2071, USA

[15]Eureka Scientific, 2452 Delmer, Suite 100, Oakland CA 96002, USA

[16]Institute for Astronomy, University of Hawai'i, 640 North A'ohoku Place, Hilo, HI 96720, USA

[17]Department of Astronomical Science, Graduate University for Advanced Studies (Sokendai), Tokyo 181-8588, Japan

[18]Department of Astronomy, Kyoto University, Kitsahirakawa-Oiwake-cho, Sakyo-ku, Kyoto, 606-8502, Japan

[19]Office of the President, Hiroshima University, 1-3-2 Kagamiyama, Hagashi-Hiroshima, 739-8511, Japan

[20]Department of Astrophysics, CAB (INTA-CSIC), Instituto Nacional de Técnica Aeroespacial, Torrejónde Ardoz, 28850, Madrid, Spain

[21]Institute of Space and Astronautical Science, Japan Aerospace Exploration Agency, Sagamihara, 252-5210, Kanagawa, Japan

[22]Jet Propulsion Laboratory, California Institute of Technology, Pasadena, CA 91109, USA

[23]TMT Observatory Corporation, 1111 South Arroyo Parkway, Pasadena, CA 91105, USA

[24]Department of Astronomy, The University of Tokyo, Hongo, Bunkyo-ku, Tokyo 113-0033, Japan

[25]Institute of Astronomy and Astrophysics, Academia Sinica, P.O. Box 23-141, Taipei 106, Taiwan

[26]Kavli Institute for the Physics and Mathematics of the Universe, The University of Tokyo, Kashiwa 277-8568, Japan

[27]Department of Cosmosciences, Hokkaido University, Sapporo 060-0810, Japan

[28]H.L. Dodge Department of Physics and Astronomy, University of Oklahoma, 440 W Brooks St Norman, OK 73019, USA

[29]Astronomical Institute, Tohoku University, Aoba, Sendai 980-8578, Japan

(e.g. Kirkpatrick 2005) at these temperatures, which is thought to indicate a transition from cloudy (L-type) to clear (T-type) photopheres (e.g. Leggett et al. 2000; Chabrier et al. 2000; Allard et al. 2001). The apparent difference between planets and brown dwarfs in this regard can be theoretically justified through a dependence of the transitional temperature on surface gravity (Metchev & Hillenbrand 2006; Marley et al. 2012).

Recently, we presented the discovery of GJ 504 b (Kuzuhara et al. 2013), a planetary companion to a nearby G0-type star, made with direct imaging as part of the 'Strategic Exploration of Exoplanets and Disks with Subaru' program (SEEDS; Tamura 2009). With an age of >100 myr and a temperature of less than 600 K, GJ 504 b allows for study of a new class of planetary atmospheres, where the clouds have largely disappeared from the photosphere, more clearly revealing the molecular contents of the atmospheres. In this paper, we present new data in intermediate-band methane filters within H-band and re-analyze the broad-band photometry from Kuzuhara et al. (2013) in order to acquire a uniformly reduced data set. In the following, we first describe the new observations that have been acquired, and the reduction procedure for the acquired data, as well as the re-reduction of the previous broad-band data. We then summarize the results, and compare them to a grid of models in order to constrain physical parameters, and finally we discuss the broader implications of our results.

2. Observations and Data Reduction

Here, we discuss the J and H-band observations that have already been presented by Kuzuhara et al. (2013), new observations in CH_4S and CH_4L, and a re-observation in K_s-band. CH_4S and CH_4L are intermediate-band methane filters ranging from 1.486 μm to 1.628 μm for the former and from 1.643 μm to 1.788 μm for the latter. These filters are designed to capture both sides of the 1.6 μm methane bandhead expected in cool giant planet atmospheres under chemical equilibrium. If strong methane absorption is present, there should be significantly more flux in the CH_4S band, which is outside of the methane absorption feature, than in the CH_4L band, which is inside of it. The CH_4S and CH_4L images were acquired on 15 May 2012 using the HiCIAO camera (Suzuki et al. 2010) with the AO188 adaptive optics system (Hayano et al. 2008) in the 2-channel SDI

(simultaneous spectral differential imaging) mode, in which the incoming beam is split into two beams using a Wollaston prism. One beam is passed through the CH_4S filter and one through the CH_4L filter, and the resulting two images are placed side by side on the detector. As with all the other observations of GJ 504, the Angular Differential Imaging (ADI; Marois et al. 2006) mode was used, where the image rotator is used to keep the orientation of the telescope pupil fixed on the detector (pupil tracking). An exposure time of 20 seconds was used for each frame, without co-adding. During the continuous sequence of 106 minutes (including overheads), 219 frames were acquired with these settings, spanning a field rotation of 94.4º. In addition, non-saturated images were acquired interspersed with the ADI sequence (50 frames in total) for photometric referencing. These used 1.5 s exposures (without co-adding) and a neutral density (ND) filter. The ND filter has a transmission of 0.859% across the broad H-band, but varies across wavelength such that the transmission is 0.714% in CH_4S and 0.929% in CH_4L. The K_s-band observation was acquired on 11 May 2012 in the same way as for the previous K_s-band measurement of Kuzuhara et al. (2013) from 28 Feb 2012, using HiCIAO in the ADI mode. Each co-added exposure consisted of 10 co-adds with individual integration times of 10.0 s. A total of 38 co-added exposures were acquired, spanning a field rotation of 68.1º. All observations used a circular occulting mask with a diameter of 0.''4.

Since the Wollaston prism splits up the beam based on polarization state, there is in principle a risk that either instrumental polarization or polarized light from the planet itself could impact the apparent photometry in the SDI imaging. However, these effects are small (note that the planetary flux is emitted light rather than reflected light), particularly as the field rotation during the observation was more than 90º, which means that any polarization effect should be efficiently averaged out across the observation. Hence, we treat these effects as negligible in this analysis.

Data reduction was performed using the ACORNS-ADI pipeline in a uniform manner, described in Brandt et al. (2013). In addition to the CH_4S, CH_4L, and K_s-band data, the J and H-band data from Kuzuhara et al. (2013) were re-reduced as well, since the discovery paper used a different pipeline and different reduction parameters and we wanted a uniform procedure. We also wished to examine whether uncertainties in the centroiding could have led to slightly higher photometric uncertainties than had previously been accounted for. Consequently, particular attention was committed to the registration procedure, which was applied after standard de-striping and flat fielding of the data. Errors in image centroiding and registration propagate into the derived companion photometry, and always result in a lower measured companion flux. An incorrect absolute centroid will dilute the companion flux in a de-rotated and collapsed image. The impact of this effect scales with the amount of field rotation during the observation. Errors in image registration reduce the measured companion photometry as shown in Figure 6 of Brandt et al. (2013); for example, root-mean-square errors of one HiCIAO pixel in both the horizontal and vertical directions reduce the measured near-IR photometry by ~20%.

The images of GJ 504 were nearly all taken with an opaque mask covering the central star, making registration and centroiding difficult: a positional shift by the star relative to the mask does not simply appear as a positional shift in the image on the detector. We therefore started out by not attempting to register the raw masked images, nor attempting to fit an absolute centroid directly. Instead, we initially assumed the frame-to-frame pointing stability to be perfect, estimated the centroid by eye, and then performed LOCI (Locally Optimized Combination of Images; Lafrenière et al. 2007). We then de-rotated the image sequence around many possible absolute centroids and co-added each resulting sequence. In this way, it becomes possible to find the centroid offset that maximizes GJ 504 b's signal-to-noise ratio in the final, reduced frame.

Our method partially compensates for a real, stable drift of the stellar centroid, by also fitting for the drift speed and direction that maximizes the companion signal-to-noise ratio. Typical centroid drifts over a long observation are generally not more than 1–2 pixels (Brandt et al. 2013), with a ~2–3 pixel drift observed over a multi-hour observation at very high airmass (Thalmann et al. 2011). We therefore expect the uncorrected bias from a stable drift to be much less than the 20% that would have been introduced by positional fluctuations of 1 pixel, as mentioned above (Brandt et al. 2013). Likewise, the actual frame-to-frame positional fluctuations in SEEDS images are small, $\lesssim 0.3$ pixels (Brandt et al. 2013) and will have little effect on our photometry.

Major variations in atmospheric conditions and AO performance over the course of an observing run present another photometric difficulty. While it is pos-

sible to estimate the data quality from the diffraction pattern on masked frames, HiCIAO does not introduce an unsaturated central peak (as would a semitransparent mask) for a more precise calibration. Unsaturated photometric frames were sometimes taken only before and after an observing sequence and sometimes interspersed within a sequence. While most observations had stable conditions and consistent photometry across the sequences, the May 2011 H-band data presented a more difficult case. The unsaturated photometric frames taken before and after the sequence of masked science frames showed a remarkable uniformity in AO performance, and the science data themselves seemed to show no major AO failures or changes in observing conditions. However, using only the first half of the sequence yielded a planet flux ∼50% higher than that derived from the latter half of the sequence. This discrepancy corresponds to a 2σ significance level. None of the other data sets showed any differences of this magnitude for companion photometry in subgroups of science frames.

All frames were subjected to a LOCI-based PSF (Point Spread Function) modeling and subtraction with standard ACORNS-ADI parameters ($N_{\mathrm{FWHM}} = 0.6$, $N_{\mathrm{Area}} = 200$). We also tried varying the parameters, but since the final image is not strongly dominated by PSF residuals at the location of the companion, this had a negligible effect. All the PSF-subtracted data were de-rotated to a common field orientation and co-added to form the final image of each filter. The primary flux (rescaled from the neutral density filter images in the case of CH_4S and CH_4L) as well as the secondary flux were calculated in circular apertures with a diameter equal to the 75% of the FWHM. Partial subtraction as a function of angular separation imposed by LOCI was accounted for when determining the contrasts.

3. Results and Discussion

The final CH_4S and CH_4L images resulting from the reduction are shown in Fig. 1, and the photometric values are shown in Table 1. It can be immediately seen from the images that the planet is bright in CH_4S but disappears in CH_4L. This corresponds exactly to the behavior expected from an atmosphere with methane absorption, given that CH_4L encompasses the methane aborption feature, whereas CH_4S represents the continuum flux. Apparent magnitudes for the companion were calculated as the measured

contrast to the primary plus the magnitude of the primary in the given filter. Since there are no literature values for the primary's CH_4S and CH_4L magnitudes, we translated the H-band magnitude into these bands by relating the stellar flux to the Vega flux in the relevant passbands, assuming blackbody radiation with a T_{eff} of 6234 K for GJ 504 (G0V) and 9602 K for Vega (A0V). As expected, the corrections were very small, with $CH_4S - H = 0.02$ mag and $CH_4L - H = -0.01$ mag. Apparent magnitudes were translated into absolute magnitudes using the parallax distance of 17.56±0.08 pc from Hipparcos (van Leeuwen 2007).

The updated J and H photometry is ∼0.1 mag brighter than the previous photometry. This is consistent within the error bars, but we adopt the new photometry as it more accurately represents the full set of flux losses possible in the reduction procedure. Our K_{s}-band photometry based on the newer (May 2012) data point alone is ∼0.3 mag fainter than previously, which is again consistent given the larger scatter in the Feb 2012 data. The K_{s}-band photometry presented here is based on a weighted mean of the two epochs[1]. We note that the changes in JHK values of this order correspond to changes of a small fraction of 1 M_{Jup} in inferred mass (∼0.1–0.2 M_{Jup}) regardless of the choice of mass-luminosity model, hence there is no significant change to the mass estimation presented in Kuzuhara et al. (2013). On this topic, it is also worth noting that the uncertainties in physical quantities from these observational uncertainties are strongly dominated by model uncertainties, as could also be seen in Kuzuhara et al. (2013). For instance, comparing the old and the new measurements within the context of the Spiegel & Burrows (2012) models, the differences in inferred temperature and luminosity are 1% and 6%, respectively. By contrast, the difference for equal measurements between the Baraffe et al. (2003) models and the Spiegel & Burrows (2012) models are 14% in temperature and 51% in luminosity. This is simply because the Spiegel & Burrows (2012) models generally predict fainter magnitudes for a given effective temperature and luminosity. We use the dominating span between the models as the uncertainties when we plot the luminosity and temperature in Figs. 2 and 3.

Using the full range in luminosity, we show in Fig. 2 that the mass estimate remains well constrained to

---

[1] We note here that the newer (May 2013) K_{s}-band image has in fact already been plotted in Kuzuhara et al. (2013).

the planetary mass range, irrespective of initial conditions. The agreement between the photometry of our new K_s-band observation with the previous one also demonstrates the general robustness of the photometry. However, one issue that should be kept in mind is that the H-band observation displays a puzzling behavior, where the companion appears to have a 2σ different brightness in the first and second halves of the data set, apparently irrespective of calibration issues. It may be that something (e.g., temporary cloud coverage) occurred during some part of the observation such that it should not be trusted. However, there are no visual or quantitative clues in the data to support such an assessment. In general, it should be recalled that the difference of the two halves of the data set could simply be a statistical fluctuation, as 2σ is not a statistically unreasonable deviation. We note that, as was mentioned by (Kuzuhara et al. 2013), the average H-band photometry of the May 2011 epoch is consistent with the photometry from the March 2011 discovery epoch, which may support the statistical fluctuation interpretation. Future observations will be necessary to conclusively settle this issue.

With the CH_4S and CH_4L observations taken simultaneously, the methane detection is robust to any photometric calibration uncertainties. The absorption is deep and appears consistent with late T-dwarfs in the field. In order to quantify this, we calculated spectral indices from brown dwarfs in the SpeX prism library[2] using CH_4S and CH_4L filter functions. A comparison to GJ 504 b is shown in Fig. 3. It can be seen that the methane absorption of the planet is consistent with spectral types later than T6. To further check how GJ 504 b compares to empirical spectra, we also calculated JHK photometry from the SpeX library in addition to CH_4S and CH_4L, and derived χ^2 after applying a best-fit scaling factor and penalizing spectra predicting a CH_4L detection (Currie et al. 2011). Examples from the comparison are shown in Fig. 4. This analysis again suggests a late spectral type, with T8 providing a better fit than earlier spectral types, although the best fit still is not impressive, due to the excess brightness at K-band of GJ 504 b relative to field dwarfs already noted in Kuzuhara et al. (2013).

Methane has otherwise remained elusive in exoplanetary atmospheres thus far. While indications of methane have been suggested for the transiting planets

[2]Maintained by Adam Burgasser at http://pono.ucsd.edu/~adam/browndwarfs/spexprism

Table 1: Photometry of GJ 504 b.

Band	GJ 504 A	GJ 504 b
J	4.11 ± 0.01 mag	19.76 ± 0.10 mag
H	3.86 ± 0.01 mag	19.99 ± 0.10 mag[a]
K_s	3.81 ± 0.01 mag	19.38 ± 0.11 mag
CH_4S	3.88 ± 0.01 mag	19.59 ± 0.12 mag
CH_4L	3.85 ± 0.01 mag	>20.62 mag (3σ)

[a]There is an apparent systematic difference between the first and second halves of the data set, see text for discussion.
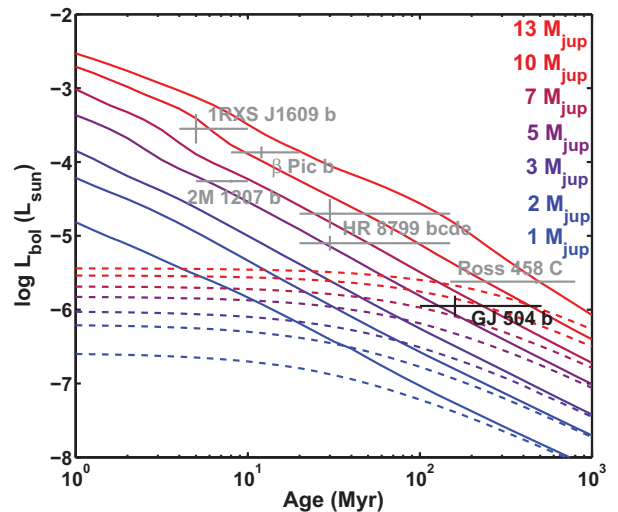

Fig. 2.— Evolution of luminosity with age as a function of mass for the coldest (dashed lines) and hottest (solid lines) initial conditions of typical warm-start models (Spiegel & Burrows 2012). The relatively old age of GJ 504 b means that it is only weakly sensitive to the initial conditions. Other objects included in the figure are β Pic b (Lagrange et al. 2010), 1RXS J1609 b (Lafrenière et al. 2010), 2M1207 b (Chauvin et al. 2005) and the HR 8799 planets (Marois et al. 2008, 2010).

HD 189733 b and WASP-12 b, these interpretations are ambiguous (e.g. Swain et al. 2008; Gibson et al. 2011; Mandell et al. 2011; Stevenson et al. 2013). Also for the case of directly imaged planets, there has been a trend of CO/CO_2 being the dominant carbon-bearing species, rather than CH_4 as is expected under chemical equilibrium (e.g. Lodders & Fegley 2002; Konopacky 2013; Lee et al. 2013, and references above). Methane absorption has been identified in the atmosphere of HR 8799 b (Barman et al. 2011), though at modest strength. A stronger case of methane absorption has been reported in Ross 458 C (Burgasser et al. 2010), which is a very wide ($\sim$1000 AU) companion to an M-dwarf binary with an inferred mass near the deuterium-burning limit. In Kuzuhara et al. (2013), we noted that the colors of GJ 504 b are similar to those of GJ 758 B (Thalmann et al. 2009), which is a similarly cold brown dwarf companion to a Sun-like star. Our current detection of methane further underlines this similarity, as GJ 758 B also features strong methane absorption (Janson et al. 2011). This strengthens the indications that GJ 504 b belongs to a different class of atmospheres than most of the previously imaged planets. The latter share similarities with L-type or L/T transition brown dwarfs, while GJ 504 b appears to have more in common with the T spectral type range. However, like GJ 758 B, it is anomalously bright in the K-band range, which could be a signature of high metallicity or possibly low surface gravity. Indeed, this feature of high K-band brightness relative to field brown dwarfs of similar temperature is a feature that is also present in other objects with indications of very low gravity, such as CFBD-SIR J214947.2-040308.9 (Delorme et al. 2012) and Ross 458 C (Goldman et al. 2010; Burningham et al. 2011, e.g.).

The similarity of GJ 504 b to late T-type objects, implying relatively little cloud coverage (although remnant clouds cannot be excluded, see e.g. Burgasser et al. 2010; Morley et al. 2012), is particularly interesting in the context that thick clouds have been inferred even for HR 8799 b, whose temperature may be as low as $\sim$800 K (e.g. Barman et al. 2011), significantly colder than the temperature of $\sim$1400 K at which brown dwarfs lose their thick clouds (e.g. Allard et al. 2001). This implies that the transition from a more to a less cloudy regime may occur somewhere in the temperature range of 600–800 K for objects in the planetary mass range, and is consistent with the predictions of Marley et al. (2012). Future detec-
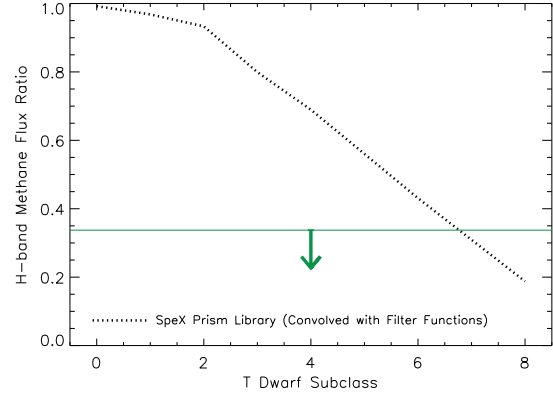

Fig. 3.— A comparison of the GJ 504 b methane flux ratio limit to the spectral type sequence of field brown dwarfs. The green horizontal line marks the measured limit of GJ 504 b. The dotted line represents our calculated indices from the SpeX prism library.
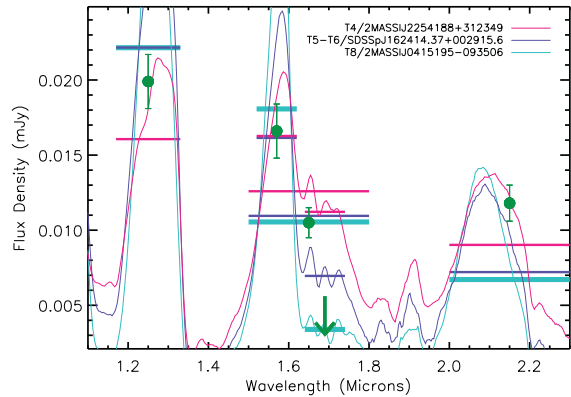

Fig. 4.— Comparison of GJ 504 b to the calculated magnitudes of field brown dwarfs from mesured spectra (McLean et al. 2003) in the Spex prism library. Only late T-type objects can reproduce the deep methane absorption seen in GJ 504 b.

tions of planets in this intermediate range would be critical to test this hypothesis. The necessary quantity of such objects may be delivered by near-future facilities such as GPI (Macintosh et al. 2008), SPHERE (Beuzit et al. 2008), or CHARIS (Peters et al. 2012). Similarly, it will be useful to study planetary mass companions to very low-mass stars and brown dwarfs (e.g. Chauvin et al. 2005), or even free-floating objects in this mass range (e.g. Delorme et al. 2012) in order to test for possible similarities or distinctions between these different populations, and thus to clarify mutual trends with surface gravity, or divergent trends from formation scenarios.

REFERENCES

Allard, F., Hauschildt, P., Alexander, D.R., Tamanai, A., & Schweitzer, A. 2001, ApJ, 556, 357

Baraffe, I., Chabrier, G., Barman, T.S., Allard, F., & Hauschildt, P. 2003, A&A, 402, 701

Barman, T., Macintosh, B., Konopacky, Q., & Marois, C. 2011, ApJ, 733, 65

Beuzit, J. et al. 2008, Proc. SPIE, 7014, 41

Bowler, B., Liu, M., Dupuy, T., & Cushing, M. 2010, ApJ, 723, 850

Brandt, T. et al. 2013, ApJ, 764, 183

Burgasser, A. et al. 2010, ApJ, 725, 1405

Burningham, B. et al. 2011, MNRAS, 414, 3590

Carson, J. et al. 2013, ApJ, 763, L32

Chabrier, G., Baraffe, I., Allard, F., & Hauschildt, P. 2000, ApJ, 542, 464

Chauvin, G., Lagrange, A.-M., Zuckerman, B, Mouillet, D., Song, I., Beuzit, J.-L., & Lowrance, P. 2005, A&A, 438, L29

Currie, T. et al. 2011, ApJ, 729, 128

Delorme, P. et al. 2012, A&A, 548, 26

Gibson, N.P., Pont, F., & Aigrain, S. 2011, MNRAS, 411, 2199

Goldman, B., Marsat, S., Henning, T., Clemens, C. & Greiner, J. 2010, MNRAS, 405, 1140

Hayano, Y. et al. 2008, Proc. SPIE, 7015E, 701510

Hinz, P., Rodigas, T., Kenworthy, M., Sivanandam, S., Heinze, A., Mamajek, E., & Meyer, M. 2010, ApJ, 716, 417

Janson, M., Bergfors, C., Goto, M., Brandner, W., & Lafrenière, D. 2010, ApJ, 710, L35

Janson, M. et al. 2011, ApJ, 728, 85

Kirkpatrick, J.D. 2005, ARA&A, 43, 195

Konopacky, Q., Barman, T.S., Macintosh, B.A., & Marois, C. 2013, Science, 339, 1398

Kuzuhara, M. et al. 2013, ApJ, 774, 11

Lafrenière, D., Marois, C., Doyon, R., Nadeau, D., & Artigau, E. 2007, ApJ, 660, 770

Lafrenière, D., Jayawardhana, R., & van Kerkwijk, M. 2010, ApJ, 719, 497

Lagrange, A.-M., et al. 2010, Science, 329, 57

Lee, J.-M., Heng, K., & Irwin, P.G.J. 2013, ApJ, accepted, arXiv:1307.1404

Leggett, S.K., Geballe, T.R., Fan, X. et al. 2000, ApJ, 536, L35

Lodders, K. & Fegley, B. 2002, Icarus, 155, 393

Macintosh, B. et al. 2008, Proc. SPIE, 7015, 43

Mandell, A., Drake, D.L., Blake, G.A., Knutson, H.A., Mumma, M.J., Villanueva, G.L., & Salyk, C. 2011, ApJ, 728, 18

Marley, M.S., Saumon, D., Cushing, M., Ackerman, A.S., Fortney, J.J., & Freedman, R. 2012, ApJ, 754, 135

Marois, C., Lafrenière, D., Doyon, R, Macintosh, B., & Nadeau, D. 2006, ApJ, 641, 556

Marois, C., Macintosh, B., Barman, T., Zuckerman, B., Song, I., Patience, J., Lafrenière, D., & Doyon, R 2008, Science, 322, 1348

Marois, C., Zuckerman, B., Konopacky, Q., Macintosh, B., Barman, T. 2010, Nature, 468, 1080

McLean, I.S., McGovern, M.R., Burgasser, A.J., Kirkpatrick, J.D., & Kim, S.S. 2003, ApJ, 596, 561

Metchev, S.A. & Hillenbrand, L.A. 2006, ApJ, 651, 1166

Morley, C.V., Fortney, J.J., Marley, M.R., Vissher, C., Saumon, D., & Leggett, S.K. 2012, ApJ, 756, 172

Peters, M.A. et al. 2012, Proc. SPIE, 8446, 7

Skemer, A.J. et al. 2012, ApJ, 753, 14

Spiegel, D.S. & Burrows, A. 2012, ApJ, 745, 174

Stevenson, K., Bean, J.L., Seifahrt, A., Desert, J.-M., Madhusudhan, N., Bergmann, M., Kreidberg, L., & Homeier, D. 2013, ApJ, submitted, arXiv:1305.1670

Suzuki, R. et al. 2010, Proc. SPIE, 7735, 101

Swain, M.R., Vasisht, G., & Tinetti, G. 2008, Nature, 452, 329

Tamura, M. 2009, in AIP Conf. Ser. 1158, Exoplanets and Disks: Their Formation and Diversity, ed. T. Usuda, M. Tamura, & M. Ishii (Melville, NY: AIP), 11

Thalmann, C., et al. 2009, ApJ, 707, L123

Thalmann, C., et al. 2011, ApJ, 743, L6

Tokunaga, A.T. et al. 1998, Proc. SPIE, 3354, 512
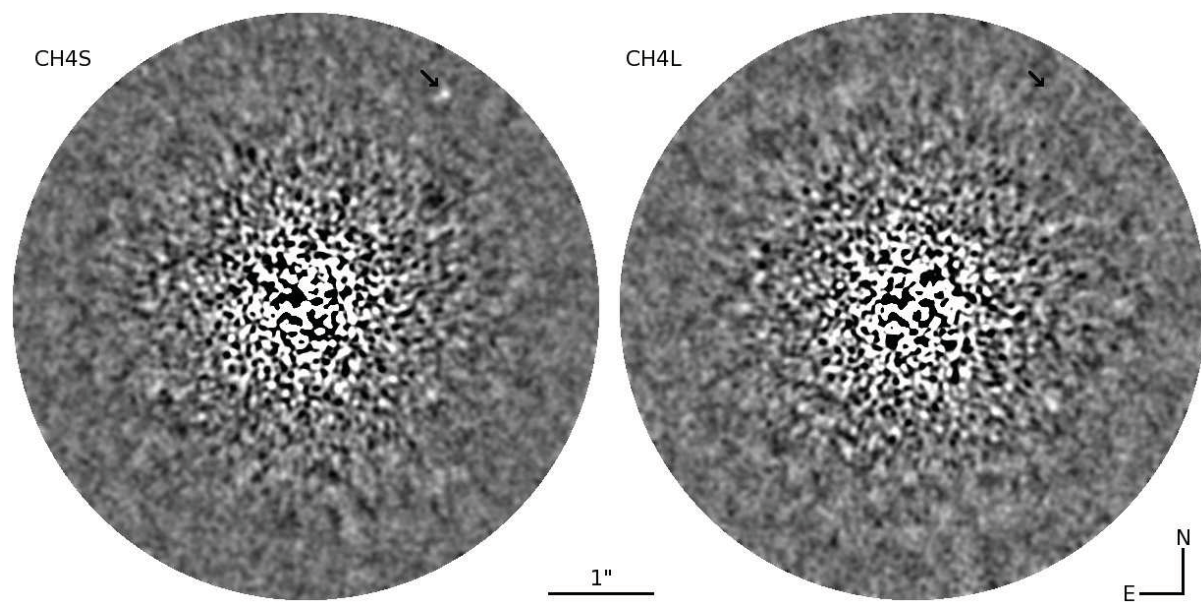
van Leeuwen, F. 2007, A&A, 474, 653

Fig. 1.— Image showing the methane absorption in GJ 504 b. Left panel: The CH_4S filter, outside of the methane absorption band. Right panel: The CH_4L filter, inside of the methane absorption band. The planet is bright in CH_4S but completely disappears in CH_4L, implying strong methane absorption.